

# Thermodynamics of Hydrogen Bond Patterns in Supramolecular Assemblies of Water Molecules

Marc Henry\*<sup>[a]</sup>

The PACHA (Partial Atomic Charges and Hardnesses Analysis) formalism is applied to various supramolecular assemblies of water molecules. After a detailed study of all available crystal structures for ice polymorphs, we show that the hydrogen bond strength is roughly constant below 1 GPa and considerably weakened above that value. New hydrogen bond patterns are proposed for ice IV, V, and VI after ⟨EB⟩ (electrostatic balance) minimization. For other polymorphs, there is an almost perfect coincidence between experimental and predicted hydrogen bond patterns. The evolution of hydrogen bond energy as a function of molecular geometry in water clusters with up to 280 water molecules and in large supramolecular compounds is quantitatively described. Inter-molecular hydrogen bonds are found to lie between  $-9$  and

$-32$  kJ mol<sup>-1</sup>, the stronger interaction occurs within the spherical fully disordered water droplet buried at the heart of Müller's superfullerene keplerate. The weakest one occurs in a chiral molecular snub cube built from six calix[4]resorcinarene and eight water molecules. Intramolecular hydrogen bonds are found in the range  $-10$ – $100$  kJ mol<sup>-1</sup> and can thus be considerably stronger than intermolecular bonds. Finally, through the investigation of a clathrate type I compound, it was possible to obtain a deep insight of the host–guest interactions and self-assembly rules of water cages in these materials.

## KEYWORDS:

bond energy · clathrates · crystal engineering · hydrogen bonds · water chemistry


## 1. Introduction

Understanding and prediction of properties of supramolecular assemblies of water molecules at a nanometer scale is a real scientific challenge for all scientists involved in physics, chemistry, physics, biology, geology, or astronomy. In physics, the molecular structure of liquid water with its fascinating random hydrogen bond network is still a subject of intensive research. Moreover, although at least 14 ice polymorphs have been identified, no systematic study of the effect of the crystalline network on the hydrogen bond strength have been performed. In chemistry, guest water clusters or even full water ladders are very often found trapped within supramolecular host architectures. In biology, nucleic acids, proteins, and enzymes are heavily hydrated to give rise to the still very mysterious long-range hydrophobic effect. In geology, solid–water interfaces are known to play a major role in rock formation and weathering processes but their quantitative molecular description is still elusive. Finally, amorphous forms of ice are commonly encountered under extraterrestrial conditions but very little information is available concerning the hydrogen bond patterns in these random networks. As far as theory may be concerned, ab initio methods are well suited for the study of small water clusters or for the investigation of periodic crystals with rather small unit cells. But they would obviously not be able to cope with Müller's "giant molecular ball", which, like a jewel case, holds a crystal-clear pearl of water made of at least 59 water molecules,<sup>[2]</sup> or with the large icosahedral clusters assumed to be present in liquid water.<sup>[3]</sup> If these objects are pretty large assemblies, they nevertheless remain quite small objects relative to a crystal. The understanding of such hydrogen-bonded networks may then

lead researchers to undertake more challenging issues in molecular tectonics, clathrate chemistry, and molecular biology.

As explained above, there is a considerable interest for a quantitative structural theory of hydrogen bonding. In a previous paper,<sup>[1]</sup> we have presented the nonempirical PACHA formalism based on a spherical approximation of DFT equations, which allows us to treat considerably larger-sized objects than what can be achieved by standard quantum mechanics computations. Therefore, it allows us to explore the domain of organization that spans from clusters to crystals, a critical scale range involved in many processes. However, providing a quantitative hydrogen bonding theory in the size domain from clusters to periodic crystal present some problems. First, most crystallographic structures contain some static disorder superimposed to their average periodic order; this should be taken into account in the algorithm. Furthermore, an accurate location of hydrogen atoms in structures requires high-quality single-crystal neutron diffraction data. As such data is rather scarce in literature, it is of considerable interest to be able to predict hydrogen atom positions by energy minimization

[a] Prof. M. Henry  
Solid-State Molecular Tectonics  
Institut Le Bel  
Université Louis Pasteur  
4, Rue Blaise Pascal, 67070 Strasbourg Cedex (France)  
Fax: (+33) 39024-1325  
E-mail: henry@chimie.u-strasbg.fr

 Supporting information for this article is available on the WWW under <http://www.chemphyschem.com> or from the author.

techniques. This is why ice polymorphs, Müller's Keplerate  $(\text{NH}_4)_{42}[\text{Mo}_{72}^{\text{VI}}\text{Mo}_{60}^{\text{V}}\text{O}_{372}(\text{AcO})_{30}(\text{H}_2\text{O})_{72}] \cdot 300\text{H}_2\text{O} \cdot 10\text{NH}_4\text{OAc}$ ,<sup>[2]</sup> or Chaplin's icosahedral clusters<sup>[3]</sup>  $(\text{H}_2\text{O})_{280}$  are fascinating cases for simulations.

It is worth to notice that our minimization procedure is not yet able to perform a full crystal structure optimization. As only torsion angles can be varied, the intramolecular geometry (bond lengths and bond angles) is completely frozen at all stages. This is an obvious limitation as usually hydrogen bonding and cooperative effects have an influence on both intra- as well as intermolecular geometry. Similarly, when clusters are extracted from crystalline networks, we completely neglect the unavoidable structural relaxation linked to surface effects. Finally, the PACHA formalism is only able to deal with enthalpic effects. For ice polymorphs, it is known that entropic contributions also play a crucial role. It is thus not possible to address the interesting problem of stability under various pressure and temperature conditions within our approach. Even though it is limited to the finding of optimum directions of hydrogen bonding within an array of frozen donors and acceptors and to the associated enthalpic effects, the proposed approach should nevertheless be quite useful in physics, chemistry, or biology because it can be used to treat, on nonempirical grounds, any kind of molecular cluster or crystalline network.

## 2. Ice Polymorphs

Earlier in this issue,<sup>[1]</sup> it was shown that the experimental hydrogen bond energy,  $E_{\text{HB}} = -22.6 \pm 2.9 \text{ kJ mol}^{-1}$ , deduced from the microwave spectrum of the  $(\text{H}_2\text{O})_2$  dimer in the gas phase,<sup>[4]</sup> was very close to the value  $E_{\text{HB}} = -22.8 \pm 1.0 \text{ kJ mol}^{-1}$  computed by insertion of the experimental geometry of the water dimer<sup>[5]</sup> into the PACHA equations. Even if the dimer is a very limited test compound, it was of crucial importance to check that we were able to reproduce quantitatively, without any adjustable parameters, the well known hydrogen bond interaction energy. Application of the same formalism to the disordered hexagonal ice network<sup>[6]</sup> has led to a predicted sublimation enthalpy  $\Delta H_{\text{subl}} = 55 \pm 5 \text{ kJ mol}^{-1}$ , which compares very favorably with the thermochemical experimental value.<sup>[1]</sup> Assuming that the total sum of van der Waals contributions for this network was  $E_{\text{vdw}} = -11.1 \text{ kJ mol}^{-1}$ , we have been able to show that the overall hydrogen bond energy was very similar in hexagonal ice ( $E_{\text{HB}} = -21.7 \pm 0.5 \text{ kJ mol}^{-1}$ )<sup>[1]</sup> and in the water dimer.

At this stage, one could ask if similar hydrogen bond energies would be obtained from the other known ice polymorphs (Figure 1).<sup>[7–16]</sup> Table 1 tries to give an answer to this question. The hydrogen bond energy was found to be, at least below 1 GPa, roughly constant at  $E_{\text{HB}} = -21 \pm 2 \text{ kJ mol}^{-1}$ . Above this value, the hydrogen bond seems to be severely weakened in good agreement with the observation that it is completely broken around 100 GPa, which leads to the symmetrical ice X network.<sup>[17]</sup> One may notice in this table that XRD does not provide enough accuracy compared to experimental data from neutron diffraction. Accordingly, ice IV, the only ice polymorph for which neutron data have not yet been collected (at least to

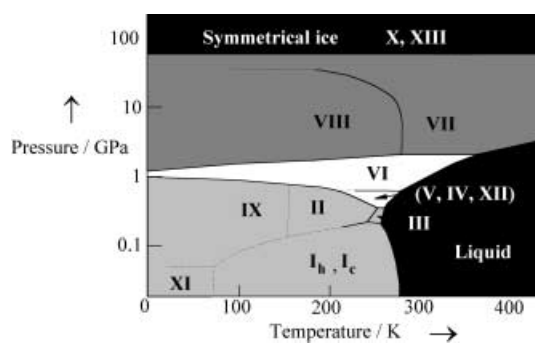


**Figure 1.** Phase diagram for ice polymorphs. Black regions correspond to domains with no structural data available. Light gray denotes constant hydrogen bond strength (same value as in the  $(\text{H}_2\text{O})_2$  dimer). The dark gray region indicates strong hydrogen bond weakening. Hydrogen bonds are broken in the symmetrical ice domain. Finally, white domains correspond to the most complex hydrogen bond patterns found in metastable polymorphs.

**Table 1.** Computed hydrogen bond strengths in known ice polymorphs. ND: Neutron diffraction, XRD: X-ray diffraction, SC: single crystal, P: powder.

Ice polymorph	Experiments	$R_{\text{val}}$	$E_{\text{HB}}$ [kJ mol <sup>-1</sup> ]
$I_h$	ND/SC, 123 K	0.069	-21.7(5)
$I_c$	ND/P, 80 K	0.095	-21.3
II	ND/SC, 213 K, 304 MPa	0.077	-22(1)
III	ND/P, 250 K, 280 MPa	0.081	-22(1)
IV	XRD/SC, 110 K	0.067	+51(55)
V	ND/P, 234 K, 500 MPa	0.012	-20(1)
VI	ND/P, 225 K, 1.1 GPa	0.103	-24(2)
VII	ND/P, 295 K, 2.6 GPa	0.026	-17.2(5)
VIII	ND/P, 10 K, 2.4 GPa	0.068	-16.4(7)
IX	ND/SC, 110 K	0.039	-21.2(2)
X	XRD/SC, 100 GPa	-	-
XI	ND/P, 5 K	0.111	-21.6(8)
XII	ND/P, 260 K, 500 MPa	0.010	-19.5(3)
XIII	XRD/SC, $P > 180 \text{ GPa}$	-	-

the best of our knowledge), shows a strongly repulsive interaction with a very large standard deviation. Due to the lack of crystallographic data for ice X and XIII we were not able to compute their electronic signatures.

The problem encountered with ice IV has prompted us to perform systematic crystal structure predictions for all ice polymorphs. Basically, all the experimental hydrogen atom coordinates were removed from the input file to leave only oxygen atoms. New hydrogen atoms were then placed in arbitrary positions to restore the neutrality of the unit cell; we used one distance constraint per hydrogen atom (OH bond length) and one constraint per water molecule (HOH bond angle). These constraints were mandatory for the PACHA formalism as we assume that the  $F$  term should not depend very much ( $F[\rho] \approx \text{constant}$ ) on the relative orientations of the water molecules. Accordingly, it is well known that this  $F$  term is mainly responsible for equilibrium bond lengths and bond angles in molecules. An amoebae downhill simplex algorithm may now be applied in order to look for a minimum value of  $\langle \text{EB} \rangle$ . During this search, torsion angles of the relative orientations of water molecules are systematically varied until the

amoebae are trapped in an energetic minimum (which may well not be a real minimum). Figures 2 and 3 show that, following this procedure, we have been able to reproduce the observed crystal structure of most ice polymorphs with an average error of 0.0099

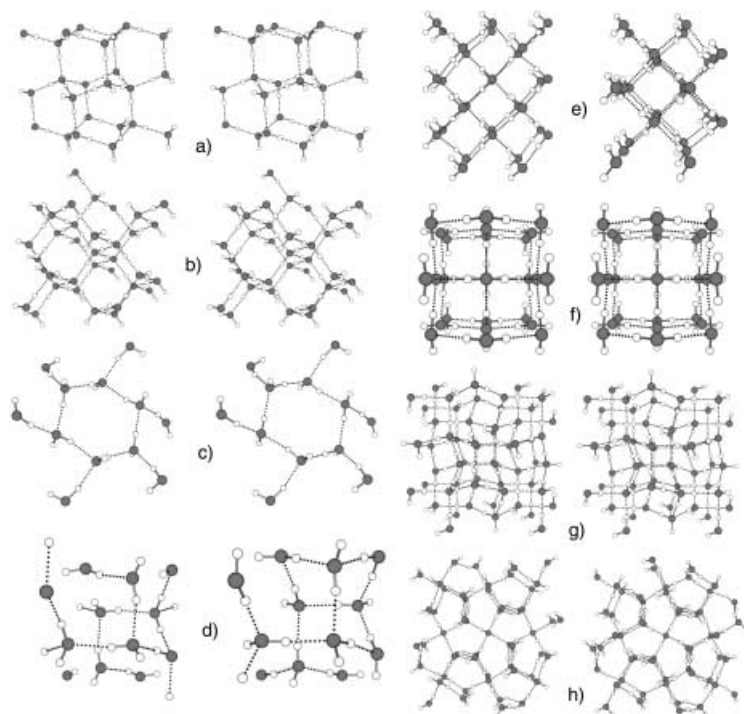


**Figure 2.** Experimental (left) and predicted (right) hydrogen bond patterns for ices a)  $I_h$ , b)  $I_c$ , c) II, d) III, e) VII, f) VIII, g) IX, and h) XII. See Figure 3 for atomic coordinates correlation.

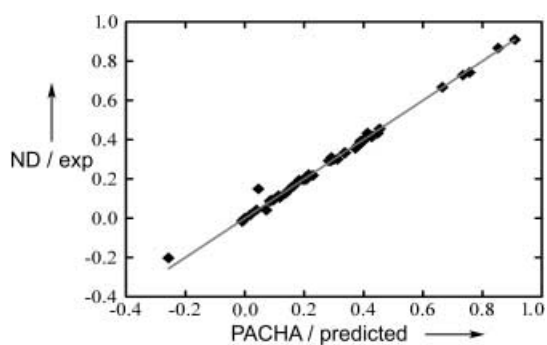


**Figure 3.** Correlation ( $r = 0.997$ ) between 54 atomic coordinates deduced from (EB) minimization procedure and experimental coordinates derived from neutron diffraction (ND) data (single crystal and powders). The average error is 0.0099, the equation of the straight line is  $\text{exp} = 0.998 \cdot \text{pred} + 0.0000$ .

for 54 hydrogen atom coordinates. This impressive correlation ( $r = 0.997$ , slope: 0.992, origin ordinate: 0.0000) between theory and neutron diffraction data confirms the validity of our initial assumption ( $F[\rho] \approx \text{constant}$ ). Six polymorphs (ice IV, V, VI, X, XI, and XIII) were however not included in this correlation. For ice IV, it would have been very surprising to find a good correlation with experimen-

tal data, as the crystal structure deduced from X-ray diffraction is obviously wrong (see Table 1). Consequently, we have not been able to find the very peculiar hydrogen bond between the two oxygen atoms above and below a puckered six-membered ring (Figure 4a). Figure 4b shows the predicted hydrogen bond pattern found for this structure after (EB) minimization. The striking difference is the absence of the threading bond and the formation of three additional hydrogen bonds per unit cell. The average hydrogen bond energy computed from this theoretical network was found to be well above that of other polymorphs:  $E_{\text{HB}} \approx -15 \text{ kJ mol}^{-1}$ . This may be an indication that the amoebae has in fact landed in a false minimum and that a better geometry should exist. Nevertheless, it is highly satisfying to see the large energy gain ( $-66 \text{ kJ mol}^{-1}$ ) relative to the experimental structure. Consequently, one has to wait for neutron data to decide if this occurrence of a threading hydrogen bond is a chemical reality. If this were the case, we would have an example of the breakdown of our assumption  $F[\rho] \approx \text{constant}$  and one would have to work out the subtle solid-state quantum-mechanical effect which affects the  $F[\rho]$  term, and which cannot be handled by our approach. Similarly, for ices V and VI, it was probably the high disorder in these rather complex structures ( $Z = 28$  and 10, respectively) which led our amoebae to a false minimum (at convergence, we get  $E_{\text{HB}} = -17.5 \text{ kJ mol}^{-1}$  for both structures). Work is in progress to see if a lower minimum can be found. For the low-temperature ordered form of hexagonal ice (ice XI), the situation was different. Here, we were able to reproduce a hydrogen bond pattern very similar to the experimental one (Figure 4g) but with a disordered model instead of an ordered one. Since we have obtained a bond isomer of the experimental structure, a direct comparison of atomic coordinates was not possible.

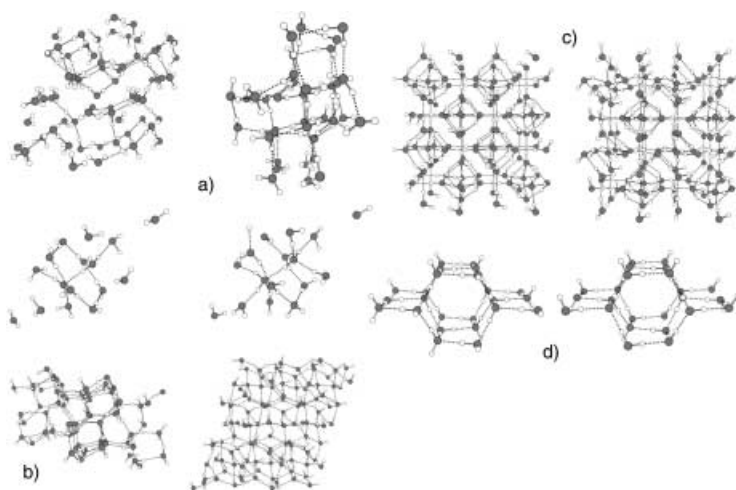


**Figure 4.** Experimental (left) and predicted (right) hydrogen bond patterns for structures where it was not possible to match the experimental atomic coordinates. a) Ice IV polymorph with its characteristic threading hydrogen bond (bottom left). b) Ice V polymorph. c) Ice VI polymorph. d) Ice XI polymorph.

### 3. Water Clusters Inside Supramolecular Architectures

#### 3.1 Müller's Super-Fullerene Keplerate

Our formalism was applied to this wonderful supramolecular object  $(\text{NH}_4)_{42}[\text{Mo}_{72}^{\text{VI}}\text{Mo}_{60}^{\text{V}}\text{O}_{372}(\text{AcO})_{30}(\text{H}_2\text{O})_{72}] \cdot 300\text{H}_2\text{O} \cdot 10\text{NH}_4\text{OAc}$ ,<sup>[2]</sup> in order to demonstrate our ability to deal with nanometer-sized objects on the same grounds as molecular or crystalline compounds. As water molecules are strongly disordered in the core of this cluster, we first applied our disorder-removal procedure to build a chemically reasonable model of the 59 interacting oxygen atoms in this cluster (Figure 5 a). As hydrogen atom coordinates are not available for such a disordered structure, a theoretical hydrogen bond pattern was computed for this cluster. We have thus looked for a minimum of the electrostatic part  $\langle \text{EB} \rangle$  of the molecular energy by means of an amoebae downhill simplex procedure and standard geometry ( $d_{\text{OH}} = 97 \text{ pm}$  and  $\theta_{\text{HOH}} = 105^\circ$ ) for all water molecules (Figure 5 c). At convergence, we have compared the  $\langle \text{EB} \rangle$  value of the whole cluster and the sum of the 59  $\langle \text{EB} \rangle$  values found for each water molecule isolated from the cluster and found  $E_{\text{HB}} = -472 \pm 2 \text{ kJ mol}^{-1}$ . Now, if we take a regular hydrogen bond identification scheme ( $\text{O} \cdots \text{O}$  distances shorter than the sum of the van der Waals radii of both partners,  $d_{\text{OO}} < 280 \text{ pm}$ ) no bonds are missed in a periodic stacking of water molecules (crystalline ice). In the present case of an aperiodic packing of water molecules, application of this "standard" cut-off value would lead (Figure 6) to the identification of only three hydrogen bonds, and thus to a

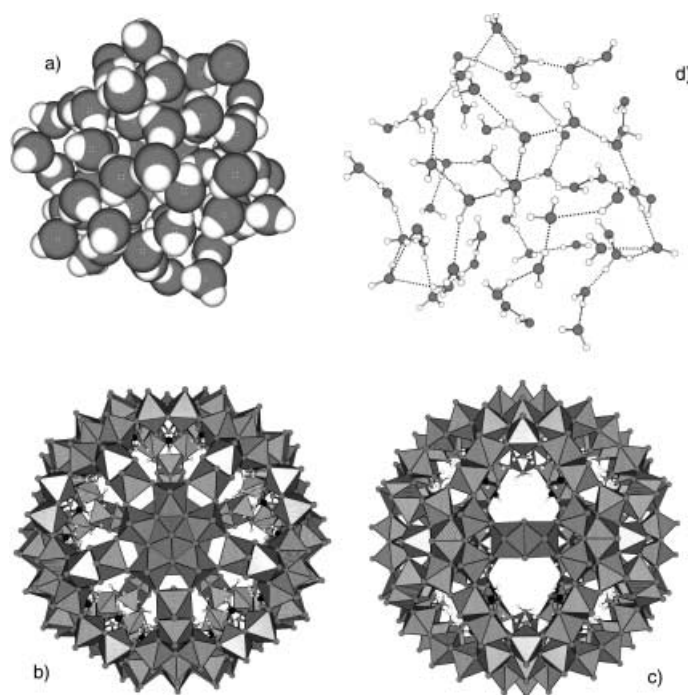


**Figure 5.** Hydrogen bond pattern in Müller's super-fullerene keplerate. a) Cluster of 59 water molecules in the spherical ball. b) Polyhedral view of the spherical shell which encapsulates the cluster along the  $C_5$  axis. c) Polyhedral view of the spherical shell encapsulating the cluster along the  $C_2$  axis. d) Theoretical pattern deduced from  $\langle \text{EB} \rangle$  minimization. The cut-off value for hydrogen bonds was  $d_{\text{OH}} < 250 \text{ pm}$  (52 bonds).

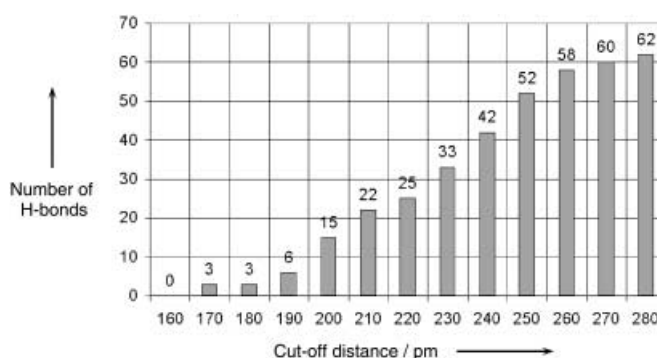


**Figure 6.** Statistical distribution of  $\text{O}-\text{H}$  distances in the cluster  $(\text{H}_2\text{O})_{59}$ .

very strong interaction energy  $E_{\text{HB}} = -472/15 \approx -157.3 \pm 0.1 \text{ kJ mol}^{-1}$ . In order to obtain a more reasonable value, closer to what is generally admitted for ice, one must increase the  $\text{O} \cdots \text{O}$  cut-off to  $310 \text{ pm}$  ( $d_{\text{OH}} < 210 \text{ pm}$ ). This leads to 22 hydrogen bonds ( $E_{\text{HB}} = -472/22 = -22 \text{ kJ mol}^{-1}$ ), but such a long distance is usually associated with van der Waals interactions rather than hydrogen bonding. Figure 6 helps to understand the origin of the problem. In this cluster, water molecules are smoothly distributed with no definite order but nevertheless are in a fully cooperative state even at quite "long" distances to produce the most stable neutral hydrogen-bonded water object ever characterized. In other words, here we have a good theoretical evidence of disordered molecular packing at the nanometer scale with an interaction energy significantly larger than fully periodic solid-state packing. A good compromise for the quantification of the hydrogen bond strength in this spherical water ball would be to use an OH cut-off value slightly higher than for ice polymorphs. Accordingly, counting all  $\text{O}-\text{H}$  distances less than  $190 \text{ pm}$  as hydrogen bonds allows us to identify 15 such bonds in the ball (Figure 6). This leads to a quite high but reasonable average energy of about  $-32 \text{ kJ mol}^{-1}$ . This rather unusual bond strength has prompted us to consider other hydrogen-bonded clusters or networks.

#### 3.2 Icelike $(\text{H}_2\text{O})_{10}$ Cluster

Consider first the icelike  $(\text{H}_2\text{O})_{10}$  molecular cluster observed in a copper-based supramolecular complex  $[\text{Cu}_2(\text{H}_2\text{O})_4\text{L}_4] \cdot n\text{H}_2\text{O}$  (Figure 7).<sup>[18, 19]</sup> Application of our model to this isolated complex with twelve intramolecular hydrogen bonds leads to an average energy  $E_{\text{HB}} = -14 \pm 2 \text{ kJ mol}^{-1}$ . In this case, to find a weaker hydrogen bond energy than in ice should not be surprising since this cluster is just a rather small fragment of the ice network. It is noteworthy that in the same compound, two linear  $(\text{H}_2\text{O})_3$  trimers hydrogen-bonded to nitrate anions can be identified. These trimers are strongly nonequivalent with  $E_{\text{HB}} = -27 \pm 3 \text{ kJ mol}^{-1}$  for the first one (atoms O2W and O5W) and  $E_{\text{HB}} = -11 \pm 1 \text{ kJ mol}^{-1}$  (atoms O3W and O6W) for the second one. These values should however be used with extreme care, as unrealistic short distances are found in these two trimers (O2W–H2W:  $86.5 \text{ pm}$  and O3W–H3W:  $78.8 \text{ pm}$ ). Neutron diffraction data would then be necessary to discuss further the case of these two

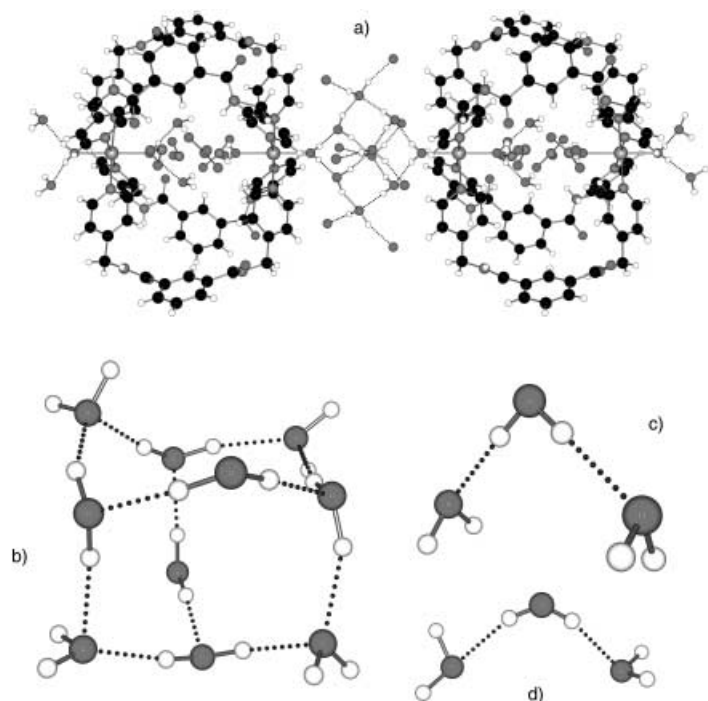


**Figure 7.** a) Icelike  $[H_2O]_{10}$  cluster in the crystal structure of  $[M_2L_4(H_2O)_4](NO_3)_4 \cdot 16H_2O$  ( $M = Cu, Ni, Co$  and  $L = 1,2$ -bis(amido-4-ethylpyridine)-benzene). b) Isolated  $[H_2O]_{10}$  cluster bridging supramolecular cages. c, d)  $[H_2O]_3$  linear trimers found inside the supramolecular cages.

trimers. We will not report the predicted hydrogen positions for this structure as it is still under investigation due to its rather large unit cell.

### 3.3 Cubelike $(H_2O)_8$ Cluster

A rather similar case is provided by the cube of water molecules identified in the crystal structure of another supramolecular coordination complex.<sup>[20]</sup> Here, we met the typical case of a compound without available hydrogen atom coordinates. Application of our optimization procedure to this molecular cube leads to the hydrogen bond pattern illustrated in Figure 8. The hydrogen bond energy for this supramolecular self-assembled cube was found to be  $-14.7 \pm 0.1 \text{ kJ mol}^{-1}$ . As expected, this energy is very similar to that obtained for the icelike decamer and significantly higher in energy than what was found for crystalline ice.

### 3.4 Ladderlike Assembly Based on Water Hexamers $(H_2O)_6$

The case of the water hexamer  $(H_2O)_6$  identified in the channels of a supramolecular organic crystal deserves special attention.<sup>[21]</sup> Firstly, it is not a free hexamer as it is engaged into a molecular ladderlike 1D network. Secondly, the crystal structure has been studied by X-ray diffraction rather than neutron diffraction. Thus, the experimentally deduced hydrogen bond pattern shows some very unusual features, such as oxygen atoms 275 pm apart without any hydrogen bond between them, and hydrogen atoms all engaged in much longer  $O \cdots N$  contacts. Insertion of

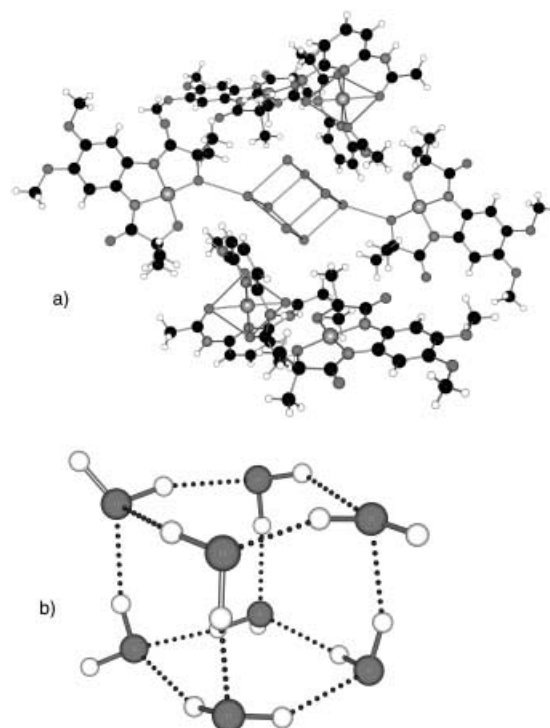


**Figure 8.** a) Molecular water cube  $[H_2O]_8$  in the crystal structure of  $[A_2B](H_2O)_8$  ( $A = \kappa^4$ -[1,2-bis(2-oxy-2-methylpropanamido)-4,5-dimethoxybenzene]cobaltate(III) and  $B = \text{bis-}\kappa^3$ -(2,6-diacetamidopyridine)cobalt(II)). b) Theoretical hydrogen bond pattern deduced from  $\langle EB \rangle$  minimization in the molecular cube of water molecule.

these X-ray data into the PACHA formalism leads to  $E_{HB} = -18 \pm 8 \text{ kJ mol}^{-1}$  for the free chairlike hexamer  $(H_2O)_6$  and  $E_{HB} = -12 \pm 5 \text{ kJ mol}^{-1}$  for the isolated decamer (Figure 9a). The rather high standard deviations reflect the low accuracy of the hydrogen atom locations. Consequently, the atomic positions of the ten nonequivalent hydrogen atoms in the unit cell were submitted to our amoebae routine. At convergence, we looked for OH distances less than 180 pm, but found no evidence of a ladderlike 1D network of water molecules. Instead, we detect the occurrence of an isolated  $(H_2O)_{10}$  decamer characterized by  $E_{HB} = -16.4 \pm 0.1 \text{ kJ mol}^{-1}$  (Figure 9b). However, if we increase our  $O \cdots H$  lookup criterion to 201 pm, we see the molecular ladder. In a more quantitative way, after a comparison between  $\langle EB \rangle$  values found for a chain containing seven decamers and for an isolated decamer we obtained  $\Delta E = -25.3 \pm 0.1 \text{ kJ mol}^{-1}$ , which means that the decamers are strongly associated within the chain.

Note that the above results were obtained after optimization of free water chains completely isolated from the organic part of the network. Consequently, one may wonder if the same geometry would still be preserved in the presence of the host matrix. We thus completely optimized the crystal structure once more taking into account the entire unit cell content. Figure 9c shows how the geometry of the decamer is affected by its insertion into the channels of the host network. For this new structure, we found  $E_{HB} = -16.9 \pm 0.1 \text{ kJ mol}^{-1}$  to show the negligible effect of the network on the intramolecular hydrogen

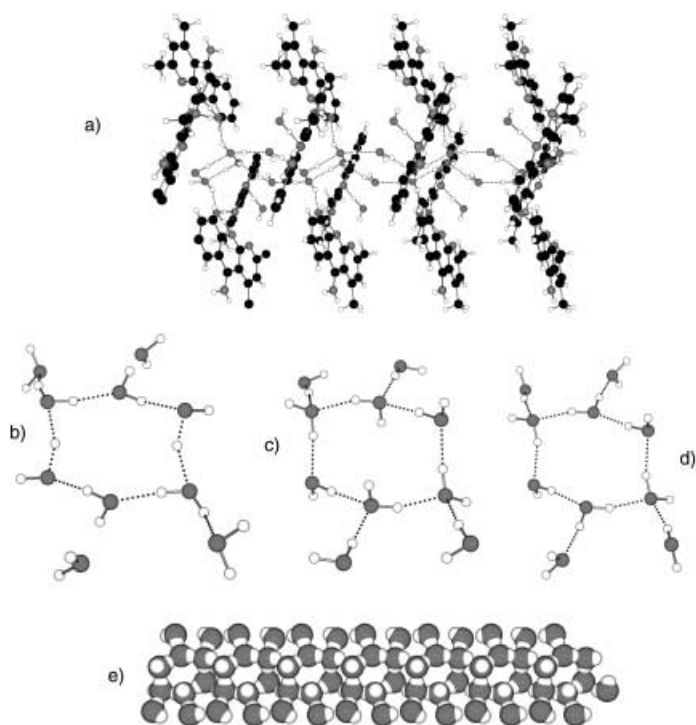


**Figure 9.** a) Ladderlike water chain in the crystal structure of 2,4-dimethyl-5-aminobenzo[b]-1,8-naphthyridine. b) Experimental XRD hydrogen bond patterns. c) Computed H-bond pattern without host network after  $\langle EB \rangle$  minimization. d) Computed hydrogen bond pattern including host network. e) Ladderlike 1D water chain obtained through stacking of the water decamers.

bridges. Concerning the ladder formation through stacking of the decamers (intermolecular bonds), we found  $\Delta E = -19.7 \pm 0.1 \text{ kJ mol}^{-1}$ . Hence, relative to a pure water chain, a hydrogen bond weakening despite shorter  $\text{O} \cdots \text{H}$  bonds (201 pm in pure water chain against 192 pm for the chain inserted in the host structure) is observed. Consequently, it appears that, upon application of a 1D periodic constraint, water molecules conspire in a much more efficient way when they are in a pure state (no constraints along the two other dimensions). As soon as periodic constraints are applied (insertion inside 1D channels), cooperation becomes less efficient due to additional interactions with the “walls” of the host structure.

### 3.5 Icosahedral Water Clusters ( $\text{H}_2\text{O}$ )<sub>280</sub>

We may also have a look at cluster structures obtained from molecular dynamics simulations. The most impressive ones were obtained by M. Chaplin when he looked for an equilibrium structure for twenty icelike ( $\text{H}_2\text{O}$ )<sub>14</sub> entities disposed at the vertices of an icosahedron (Figure 12).<sup>[3]</sup> We have thus investigated both the expanded (ES, Figure 10a) and compacted structures (CS, Figure 10b) to compare the hydrogen bond strength in these clusters to the previously derived values for ice polymorphs and smaller clusters. For the expanded structure with radius 13.3 Å, density  $\rho = 0.86 \text{ g cm}^{-3}$ , and 500 hydrogen bonds, we obtained on average  $\langle E_{\text{HB}} \rangle = -16.8 \text{ kJ mol}^{-1}$ , to be compared with  $\langle E_{\text{HB}} \rangle = -15.7 \text{ kJ mol}^{-1}$  for the more dense

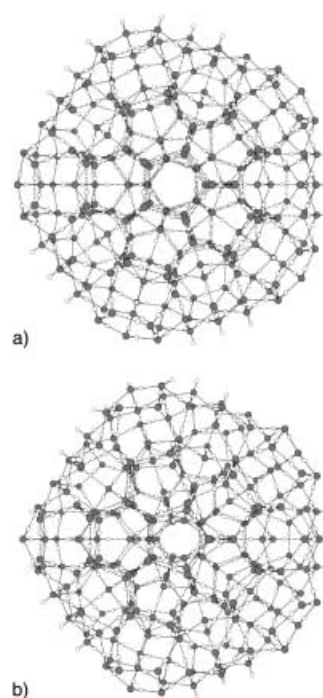


**Figure 10.** Icosahedral  $[\text{H}_2\text{O}]_{280}$  water clusters: a) expanded form and b) compact form.

polymorph ( $r = 12.9 \text{ \AA}$ ,  $\rho = 0.94 \text{ g cm}^{-3}$ ). These values are very close to those found in other ordered water clusters, but cannot compete with values found for Müller’s spherical water ball ( $r = 9.6 \text{ \AA}$ ,  $\rho = 0.48 \text{ g cm}^{-3}$ ,  $\langle E_{\text{HB}} \rangle = -32 \text{ kJ mol}^{-1}$ ). Moreover, the fact that the hydrogen bond strength is weaker in the dense polymorph than in the expanded one is also well in line with the rather low density and maximum hydrogen bond strength observed for the spherical water ball.

## 4. Hybrid Organic–Inorganic Supramolecular Assemblies

### 4.1 Self-Assembled Hybrid Molecular Polyhedra

We are also able to consider many complex self-assembled organic supramolecular aggregates. A very attractive one was found built from six calix[4]resorcinarene and eight water molecules  $[\text{C}_{32}\text{H}_{32}\text{O}_8]_6[\text{H}_2\text{O}]_8$ , which displayed the topology of a snub cube (Figure 11).<sup>[22]</sup> This chiral polyhedron has six square faces (here: calixarene molecules) linked by 32 equilateral triangles (here: water molecules). First, a slight energetic non-equivalence was found between the two chiral calixarene molecules ( $6.4 \text{ kJ mol}^{-1}$  in favor of the *S* enantiomer). The achiral isomer and the *R* enantiomer were found to be very close in energy. The average hydrogen bond strength responsible for the self-assembly was found to be  $-8.6 \text{ kJ mol}^{-1}$  (60 hydrogen bonds within the snub cube). This significant weakening of the hydrogen bond energy is obviously linked to the replacement of water molecules by much bigger calix[4]resorcinarene molecules. It may also be interesting to compare the  $\langle EB \rangle$  values of an isolated supramolecular aggregate to the one that

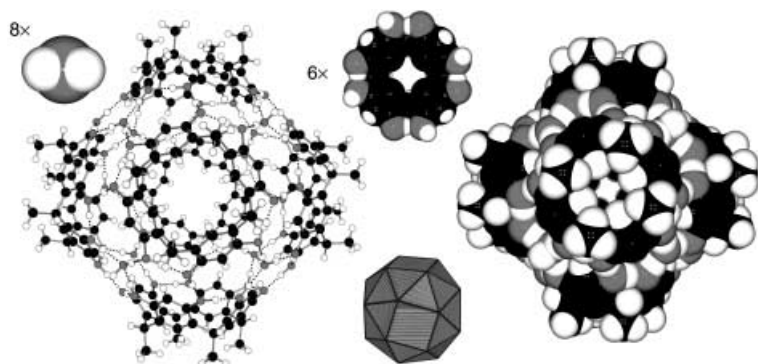


**Figure 11.** A chiral supramolecular snub cube built from eight water and six calix[4]-resorcinarene molecules.

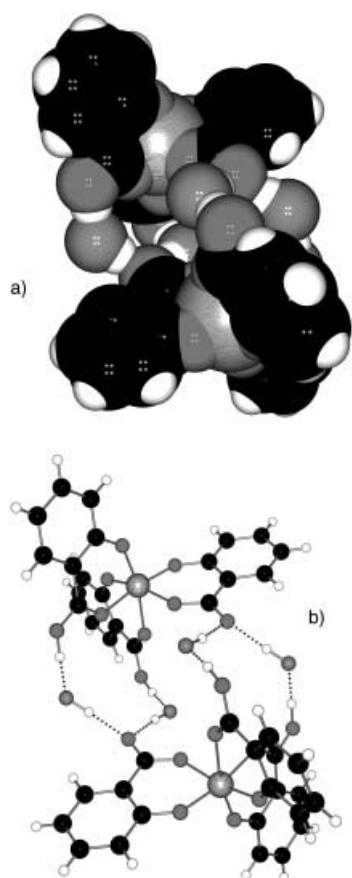


**Figure 12.** Very strong hydrogen bond pattern in the molecular complex ( $\Delta \cdot \Delta$ )- $\{Ti(sal)(salH)_2\} \cdot 2^n BuOH\}_2$ , sal: salicylic acid. a) CPK model for the complex. b) Theoretical pattern deduced from (EB) minimization (aliphatic chains for butanol molecules have been removed for clarity).

characterizes the stacking of such objects according to  $I432$  space group symmetry. In fact, it was found that nothing was gained by this stacking, the isolated aggregate is lower in energy than the whole network by  $10 \text{ kJ mol}^{-1}$ . This shows that something is probably missing which must be responsible for the network formation. Accordingly, solvent molecules (water and nitrobenzene) trapped within the  $I432$  solid-state packing interstices may be detected through X-ray diffraction.<sup>[22]</sup> This

result may explain why additional solvent molecules are absolutely needed for crystallization to occur.

#### 4.2 Organometallic Complexes

This example was selected to show that playing with hydrogen bonds in organic media does not always mean weaker hydrogen bonds. A good example is provided by a neutral tris-chelate titanium(IV) complex recently synthesized in our laboratory.<sup>[23]</sup> Due to the extremely short O...O distances (250 and 255 pm between butanol and salicylic acid molecules) and to the presence of a strong positive charge,  $q(Ti) \approx +3$ , in the neighborhood of the hydrogen bridges, it seemed that we had good evidence for a rather strong hydrogen bond. This was indeed the case, as the value derived from the optimized hydrogen bond pattern (Figure 12a) was found to be  $E_{HB} = -23.2 \pm 0.1 \text{ kJ mol}^{-1}$ . For a complex without any water molecules this is quite a high value, but we are still not able to reach the absolute record established by Müller's nanosized water droplet. Figure 13a shows another interesting case with intramolecular hydrogen bonds in a hybrid organic-inorganic divergent association of six 2,6-bis(hydroxymethyl)-*p*-cresol ligands ( $H_3BHMPC$ ) around a  $Ti_4O_2$  core (doubly fused calix[3] shape).<sup>[24]</sup> Here, by rotating the two OH groups of the chelating  $[H_2BHMPC]^-$  ligand and the free OH group of the chelating bridging  $[HBHMPC]^{2-}$  ligand around the  $-H_2C-O-$  bonds, one may probe the relative strength of these intramolecular hydrogen bond interactions. Figure 13b shows the rather deep potential well ( $E_{HB} = -98 \text{ kJ mol}^{-1}$ ) for the hydrogen atom which bridges the chelating arm of one  $[H_2BHMPC]^-$  ligand with the free OH group of one chelating bridging  $[HBHMPC]^{2-}$  ligand. The rather high value of this intramolecular hydrogen bond obviously comes from the very short O...O distance (252 pm) between both partners associated to the close proximity (284 pm) of a high positive charge on Ti atoms. The effect of the presence of the Ti atom is clearly evidenced by the curve concerning the free OH group of the chelating bridging  $[HBHMPC]^{2-}$  partner (Figure 13c). Here, the hydrogen bond strength is smaller by a factor of two ( $E_{HB} = -58 \text{ kJ mol}^{-1}$ ) with a considerable flattening of the potential well. Finally, the weakest interaction involves the free arm of the  $[H_2BHMPC]^-$  chelating ligand, which is hydrogen bonded ( $E_{HB} = -9 \text{ kJ mol}^{-1}$ ) to one of the two chelating arms of a  $[BHMPC]^{3-}$  ligand (Figure 13d). Here, the much longer  $H \cdots Ti$  and  $O \cdots O$  distances (355 and 277 pm respectively) explain the very strong weakening of the hydrogen bond interaction.

These examples illustrate the remarkable plasticity of the hydrogen bond, which for the same neutral molecular species may be as weak as  $-10 \text{ kJ mol}^{-1}$  or as strong as  $-100 \text{ kJ mol}^{-1}$  depending on the local geometry. In a forthcoming paper, we will show that in fact for water molecules hydrogen-bonded to inorganic anions or cations, a still larger energetic range ( $-10$ – $150 \text{ kJ mol}^{-1}$ ) may be spanned. These numbers again draw our attention towards the remarkable cooperation between confined water molecules inside the nanometer spherical water bowl found at the heart of the keplerate polyanion. Here, the

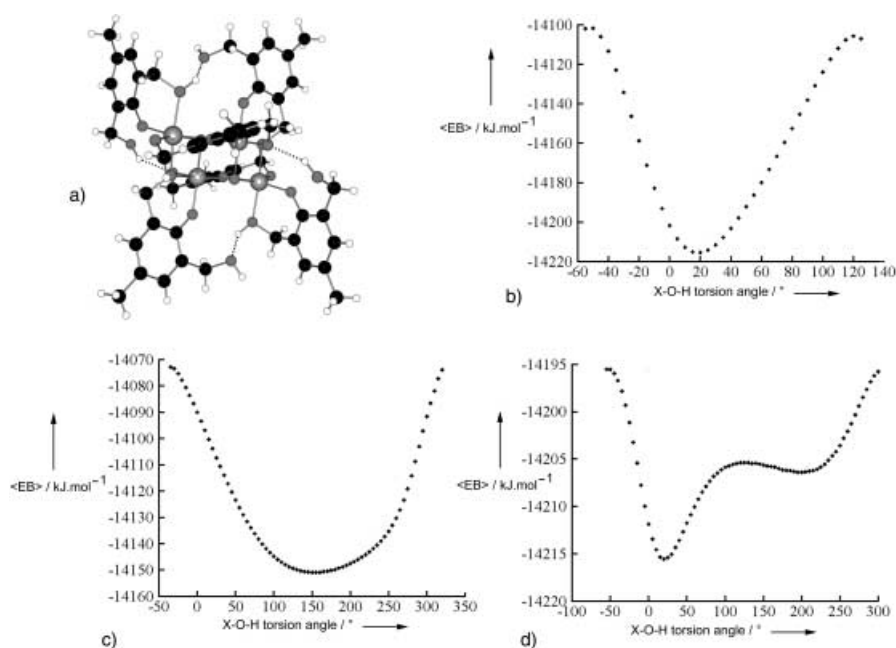


**Figure 13.** a) Intramolecular hydrogen bonds in a titanium-based hybrid organic–inorganic doubly fused calix[3]-2,6-hydroxymethyl-p-cresol. b) Topology of the hydrogen bond energy for the chelating arm of the  $[H_2BHMPC]^- - [HBHMPC]^{2-}$  pair. c) Topology of the hydrogen bond energy for the free arm of the  $[H_2BHMPC]^- - [HBHMPC]^{2-}$  pair. d) Topology of the hydrogen bond energy for the free arm of the  $[H_2BHMPC]^- - [HBHMPC]^{2-}$  pair.

cluster is just pure low-density water and no interactions with surrounding ionic species can be invoked to explain the very significant increase in hydrogen bond strength relative to other ordered water clusters or to ice polymorphs.

### 4.3 Clathrate Hydrate Structures

Finally, we turn our attention towards the most interesting class of crystalline compounds, clathrate hydrates, which are able to mix, at a molecular scale, water molecules and hydrophobic species. These clathrate hydrates raise a lot of fundamental questions: What is the relative order of magnitude between inclusion energy and hydrogen bond energy? Is the water molecule more, or less, tightly bonded in these clathrates than in ice polymorphs or in water clusters? As crystalline periodic materials, can clathrates compete with the cooperative interactions evidenced for non-periodic stacking? We have looked for an answer to these fundamental questions by studying a well and recently characterized clathrate compound  $(CH_3)_8(H_2O)_{46}$ .<sup>[25]</sup> Work is in progress for other types of cages and will be reported elsewhere. The average inclusion energy in this kind of compounds may be readily evaluated by two kinds of Madelung summations: a first one involving the host–guest combination and a second one after complete removal of the guest species. In the present case, we found as expected a rather low, hopefully negative, energy of interaction:  $E_{\text{incl}} = -1.4 \pm 0.1 \text{ kJ mol}^{-1}$ . This value points to typical

attractive van der Waals interaction between the host and the guest. Using an empty network, we next compared its  $\langle EB \rangle$  value to the sum obtained from 46 noninteracting isolated water molecules with exactly the same geometry. The result was  $E_{\text{HB}} = -22.0 \pm 0.2 \text{ kJ mol}^{-1}$ . This value, very similar to the one derived from hexagonal ice or from the vapor dimer, shows that hydrogen bonds in water clusters, ice, and in clathrate hydrates are basically of the same nature. Note that this reasonable conclusion has nothing to do with subjective feelings sustained by a long-time chemical experience. It is an objective result obtained from a precise question asked to the molecular structure or to the crystalline framework through the PACHA formalism. In particular, there is no need to make assumptions about the kind of interaction at work in a given chemical architecture. Just ask the crystal structure and you will get a useful answer expressed within the frame of the spherical approximation of DFT equations. To illustrate this point further on, note that, at a

molecular scale, type I clathrate structures are made by stacking dodecahedral cages  $(H_2O)_{20}$  with tetrakaidecahedral ones  $(H_2O)_{24}$  through face sharing between polyhedra (Figure 14). A methane molecule is trapped in both kinds of cages. This molecular view raises quite new interesting questions. What is the degree of equivalence of the two cages in terms of host–guest inter-

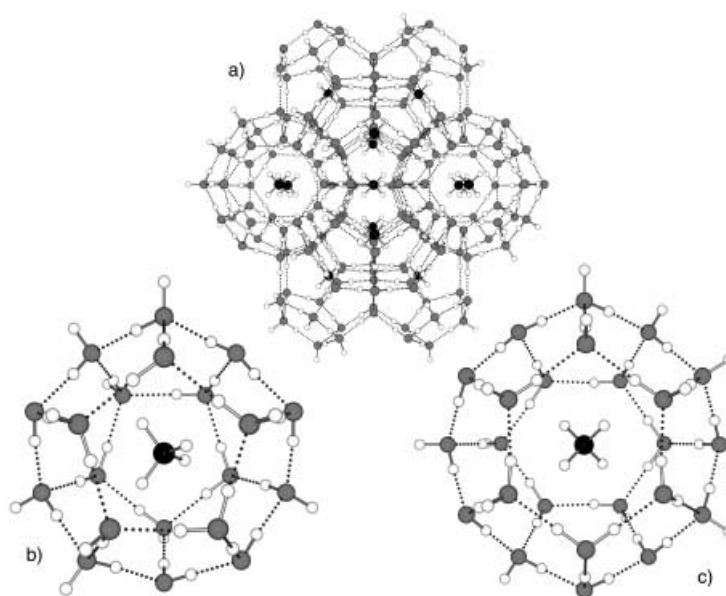


**Figure 14.** Crystal structure of the type I clathrate hydrate. Face sharing between water cages with trapped methane molecules: b) the dodecahedral cage, c) the tetrakaidecahedral cage.

actions and in terms of hydrogen bonding interactions? Is the energy associated to face sharing between polyhedra stronger or weaker than the energy associated to vertex associations along polyhedral edges? Concerning host–guest interactions, the answer is easily obtained through a comparison between the free isolated methane molecules and the two molecular cages that may be extracted from the network. The result obtained was completely unambiguous with  $E_{\text{incl}} = -1.7 \pm 0.1 \text{ kJ mol}^{-1}$  for the dodecahedral cage and  $E_{\text{incl}} = +0.3 \pm 0.1 \text{ kJ mol}^{-1}$  for the tetrakaidecahedral one. Here, the interaction energy of the whole network ( $-1.4 \text{ kJ mol}^{-1}$ ) was found to be equal to the summed energies of isolated molecular species. One may then conclude that the encapsulation process is truly a molecular process (with a clear preference for the dodecahedral site) and not a solid-state effect. Let us now try to look for a discrimination between the 92 hydrogen bonds found in the unit cell. A comparison between the two isolated  $(\text{H}_2\text{O})_{20}$  or  $(\text{H}_2\text{O})_{24}$  cages and an assembly of noninteracting similar water molecules gave  $E_{\text{HB}}(\text{H}_{40}\text{O}_{20}) = -19.6 \pm 0.2 \text{ kJ mol}^{-1}$  and  $E_{\text{HB}}(\text{H}_{48}\text{O}_{24}) = -20.3 \pm 0.2 \text{ kJ mol}^{-1}$ . Nothing can be said about this hardly significant difference. Turning now to the hydrogen bonds responsible for face sharing, we obtained an unambiguous answer  $E_{\text{HB}}(\text{faces}) = -26.1 \pm 0.4 \text{ kJ mol}^{-1}$ . These results provide us with a deep insight into the self-assembly process responsible for the formation of these clathrate structures. Basically, weaker hydrogen bonds relative to ice seem to occur in individual molecular cages. However, stronger hydrogen bonds are formed during the face sharing in the solid state. This very fortunate energetic compensation shows why, despite very different interactions at a molecular scale, no difference is observed on average between ice and clathrate structures.

## 5. Summary and Outlook

We are now in a better position to interpret the surprising result obtained with Müller's spherical nonperiodic nanosized droplet. Basically, hydrogen bond interactions are probably maximized through the simultaneous use of all kinds of symmetry elements (mirrors and rotation axes with no limitation on the order, which may be 5, 7, or even higher). For tiny clusters, obviously not all kinds of symmetry elements can be present and the hydrogen bond energy should thus not be very high. For a large enough assembly (nanometer scale), all kinds of symmetry elements can be locally present, which leads to an aperiodic object with a maximum hydrogen bond energy. At a still higher scale, translation symmetry operators become competitive with respect to point symmetry operators. The appearing of these new symmetry elements leads to a strong reduction of the possible point symmetry orders (only 1, 2, 3, 4, and 6 are now allowed). Consequently, the average hydrogen bond energy should decrease as was observed in this work. If these deductions are correct, then the disordered nanometer scale, with optimum interaction energy, should occupy a central and crucial role for most natural phenomena. This has already been known for quite a long time in biological sciences. It could now also explain the current growing interest for nanotechnology in physical and chemical sciences.

Finally, we would like to put this work in perspective with other theoretical approaches of hydrogen bonding. First, our approach can be viewed as a direct extension of Pauling's views of chemical bonding. As soon as 1939, this pioneer of the hydrogen bond concept said: "The attraction of the two atoms observed in hydrogen bond formation must be due largely to ionic forces."<sup>[26]</sup> After this study, mainly based on electronegativity and electrostatic balance concepts, we agree completely with this ingenious intuition. In fact, our sole contribution has been to put on quantitative nonempirical grounds this very simple and beautiful idea. This work is also particularly well suited for crystal engineering, which has been defined as "the understanding of intermolecular interactions in the context of crystal packing and the utilisation of such understanding in the design of new solids with desired physical and chemical properties."<sup>[27]</sup> Here, we have described an efficient algorithm for quantification and thus for a good understanding of these interactions. The paradigm of supramolecular chemistry, the identification of the dominant supramolecular interactions and understanding of their relative importance,<sup>[28]</sup> is now accessible in a routine way from the sole knowledge of molecular or crystalline structure. Can we use this knowledge to design new materials? This brings us to the computational chemist's dream: Are we really able to predict crystal structures? Here, we have shown that as far as only hydrogen atoms are concerned, the answer is no doubt "yes". We have been able to propose alternative models for the crystal structure of ice IV or the ladderlike water chain and give atomic coordinates for the molecular water cube or for Müller's water droplet. These detailed predictions should be checked against neutron diffraction data, which are not yet recorded. Consequently, the statement by A. Gavezotti:<sup>[29]</sup> "Quantum chemical methods are still intrinsically unable to describe the fine detail of weak intermolecular interactions while taking into account the full three dimensional structure of a crystal made of a reasonably sized (30–50 atoms) organic molecule" should be taken with caution. It is correct if one speaks of a full structure prediction involving all atoms in the unit cell, a task which has been done only for the ice VII, VIII, and X family<sup>[30, 31]</sup> or for ice I<sub>h</sub>.<sup>[32]</sup> It is not so true if we seek to predict probable hydrogen atom coordinates within an array of fixed acceptors (this work). In this case, even if our approach remains largely approximate (spherical charge distribution around nuclei), it is nevertheless based on rigorous quantum mechanical methods (density functional theory). In fact, our success is based on the encapsulation of these fundamental laws through the use of Allen's electronegativity scale,<sup>[33, 34]</sup> and ab initio atomic radii.<sup>[35]</sup> It is our feeling that with this study, we fill a gap by providing a secure bridge between the ab initio community (who performs a first-principles approach of chemical reality on simplified models) and synthetic chemists (who seek for quick quantitative answers concerning real chemical objects). A very nice example of this complementary aspect lies in the fact that, in 1969, L. C. Allen was the first to study the hydrogen bond by ab initio methods.<sup>[36]</sup> More than thirty years later, without the publication of his electronegativity scale,<sup>[33, 34]</sup> the presented results would never have been obtained. This work displays also some interesting links with dynamic models of liquid water structure. Thus by showing that

hydrogen bond interactions within a disordered array of water molecules are more efficient than inside an equivalent periodical array, we bring strong support to the percolation model (hydrogen-bonded network or "gel") for liquid water.<sup>[37]</sup> Similarly, we were able to give a theoretical justification to the use of a hydrogen charge  $q_{\text{H}} \sim +0.2$  in the five-site TIP5P model to allow significant improvements in the prediction of various liquid water anomalies.<sup>[38]</sup> These results obviously open new perspectives for people in need of realistic charge distributions to perform Monte Carlo or molecular dynamics simulations. Better potential functions fully compatible with ab initio atom-atom potentials should then be available soon.<sup>[39]</sup> Our new procedure should also be of considerable help for people concerned with crystal structure determination from powder techniques. By providing the computer with a nonarbitrary structural input derived from (EB) minimization, least-squares fitting procedures should converge more efficiently towards a chemically reasonable solution, even for compounds with large unit cells. Other extremely exciting perspectives are opened in biology. Consequently, the numerous fascinating hydrogen-bonded network patterns found in biology,<sup>[40]</sup> the three forms of DNA (A, B, and Z) or the various forms of RNA molecules are evident objects for further studies. Establishing realistic structural models for the hydration shell of DNA, or for the water pockets in enzymes would also be of considerable interest. Furthermore, with the future emergence of quantitative structural models for solid-water interfaces, one may hope to treat long-range chemical forces which arise from cooperative interactions allowed by unusual spatial dispositions of atoms at a nanometer scale.<sup>[41]</sup> Interesting results should then be expected in the field of colloidal chemistry and more particularly in biomineralization processes.<sup>[42]</sup>

*The author wants to associate to this work the names of Dr. Francis Taulelle and Prof. Wais Hosseini for many fruitful discussions and their constant moral and financial support.*

- [1] M. Henry, *ChemPhysChem*. **2002**, *3*, 561–569.  
 [2] A. Müller, E. Krickemeyer, H. Bögge, M. Schmidtman, F. Peters, *Angew. Chem.* **1998**, *110*, 3567–3571; *Angew. Chem. Int. Ed.* **1998**, *37*, 3359–3363.  
 [3] M. Chaplin, *Biophys. Chem.* **1999**, *83*, 211–221.  
 [4] R. S. Fellers, C. Leforestier, L. B. Braly, M. G. Brown, R. J. Saykally, *Science*, **1999**, *284*, 945–948.  
 [5] J. A. Odutola, T. R. Dyke, *J. Chem. Phys.* **1980**, *72*, 5062–5070.  
 [6] S. W. Peterson H. A. Levy, *Acta Crystallogr.* **1957**, *10*, 70–76.  
 [7] Ice I<sub>c</sub>: G. P. Arnold, E. D. Finch, S. W. Rabideau, R. G. Wenzel, *J. Chem. Phys.* **1968**, *49*, 4365–4369.  
 [8] Ice-II: B. Kamb, W. C. Hamilton, S. J. la Placa, A. Prakash, *J. Chem. Phys.* **1971**, *55*, 1934–1945.  
 [9] Ice III: J. D. Londono, W. F. Kuhs, J. L. Finney, *J. Chem. Phys.* **1993**, *98*, 4878–4888.  
 [10] Ice IV: H. Engelhardt, B. Kamb, *J. Chem. Phys.* **1981**, *75*, 5887–5899.  
 [11] Ice V: C. Loban, J. L. Finney, W. F. Kuhs, *J. Chem. Phys.* **2000**, *112*, 7169–7180.  
 [12] Ice VI, Ice VIII: W. F. Kuhs, J. L. Finney, C. Vettier, D. V. Bliss, *J. Chem. Phys.* **1984**, *81*, 3612–3623.  
 [13] Ice VII: J. D. Jorgensen, T. G. Worlton, *J. Chem. Phys.* **1985**, *83*, 329–333.  
 [14] Ice IX: S. J. la Placa, W. C. Hamilton, B. Kamb, A. Prakash, *J. Chem. Phys.* **1973**, *58*, 567–580.  
 [15] Ice XI: A. J. Leadbetter, R. C. Ward, J. W. Clark, P. A. Tucker, T. Matsuo, H. Suga, *J. Chem. Phys.* **1989**, *90*, 4450–4453.  
 [16] Ice XII: C. Lobban, J. L. Finney, W. F. Kuhs, *Nature* **1998**, *391*, 268–270.  
 [17] P. Loubeyre, R. Le Toullec, E. Wolanin, M. Hanfland, D. Hausermann, *Nature* **1999**, *97*, 503–506.  
 [18] L. J. Barbour, G. W. Orr, J. L. Atwood, *Nature* **1998**, *393*, 671–673.  
 [19] L. J. Barbour, G. W. Orr, J. L. Atwood, *J. Chem. Soc. Chem. Commun.* **2000**, 859–860.  
 [20] W. B. Blanton, S. W. Gordon-Wylie, G. R. Clark, K. D. Jordan, J. T. Wood, U. Geiser, T. J. Collins, *J. Am. Chem. Soc.* **1999**, *121*, 3551–3552.  
 [21] R. Custelcean, C. Afloroaei, M. Vlassa, M. Polverejean, *Angew. Chem.* **2000**, *112*, 3224–3226; *Angew. Chem. Int. Ed.* **2000**, *39*, 3094–3096.  
 [22] L. R. MacGillivray, J. L. Atwood, J. L. Nature, **1997**, *389*, 469–472.  
 [23] K. Gigant, A. Rammal, M. Henry, *J. Am. Chem. Soc.* **2001**, *123*, 11 632–11 637.  
 [24] A. Rammal, F. Brisach, M. Henry, *J. Am. Chem. Soc.* **2001**, *123*, 5612–5613.  
 [25] C. Gutt, B. Asmussen, W. Press, M. R. Johnson, Y. P. Handa, J. S. Tse, *J. Chem. Phys.* **2000**, *113*, 4713–4721.  
 [26] L. Pauling, *The Nature of Chemical Bond*, 3rd. ed., Cornell University Press, New York, NY, **1960**, p. 449  
 [27] G. R. Desiraju, *Crystal Engineering*, Elsevier, Amsterdam, **1989**.  
 [28] M. J. Krische, J.-M. Lehn, *Struct. Bonding (Berlin, Ger.)* **2000**, *96*, 3–29.  
 [29] A. Gavezzoti, *Crystallogr. Rev.* **1998**, *7*, 5–121, p. 93.  
 [30] C. Lee, D. Vanderbilt, K. Laasonen, R. Car, M. Parinello, *Phys. Rev. B* **1993**, *47*, 4863–4872.  
 [31] L. Ojamäe, K. Hermansson, R. Dovesi, C. Roetti, V. R. Saunders, *J. Chem. Phys.* **1994**, *100*, 2128–2138.  
 [32] I. Morrison, J. C. Li, S. Jenkins, S. S. Xantheas, M. C. Payne, *J. Phys. Chem. B*, **1997**, *101*, 6146–6150.  
 [33] J. B. Mann, T. L. Meek, L. C. Allen, *J. Am. Chem. Soc.* **2000**, *122*, 2780–2783.  
 [34] J. B. Mann, T. L. Meek, E. T. Knight, J. F. Capitani, L. C. Allen, *J. Am. Chem. Soc.* **2000**, *122*, 5132–5137.  
 [35] J. T. Waber, D. T. Cromer, *J. Chem. Phys.* **1965**, *42*, 4116–4123.  
 [36] P. A. Kollman, L. C. Allen, *J. Chem. Phys.* **1969**, *51*, 3286–3293.  
 [37] H. A. Stanley, J. Texeira, *J. Chem. Phys.* **1980**, *73*, 3404–3422.  
 [38] M. W. Mahoney, W. L. Jorgensen, *J. Chem. Phys.* **2000**, *112*, 8910–8922.  
 [39] M. A. Spackman, *J. Chem. Phys.* **1986**, *85*, 6579–6601.  
 [40] G. A. Jeffrey, *An Introduction to Hydrogen Bonding*, Oxford University Press, New York, NY, **1997**.  
 [41] S. Hyde, S. Andersson, K. Larsson, Z. Blum, T. Landh, S. Lidin, B. W. Ninham, *The Language of Shape*, Elsevier, Amsterdam, **1997**.  
 [42] S. Mann, *Nature* **1993**, *365*, 499–505.

Received: January 14, 2001 [F 361]